arXiv:astro-ph/9910416v1 22 Oct 1999

ELECTRON INJECTION BREAK AND PAIR CONTENT OF QUASAR JETS

M. Błażejowski [1], M. Sikora [1], R. Moderski [2,1], T. Bulik [1]

1) N. Copernicus Astronomical Center, Warsaw, Poland
2) JILA, University of Colorado, Boulder, USA

ABSTRACT We study the dependence of nonthermal radiation spectra in OVV quasars on location of the low energy break in the electron/positron injection function. We show that the high energy spectra produced during the outbursts are presumably superposed from two components, one resulting from Comptonization of emission lines, which dominates at MeV-GeV energies, and the other resulting from Comptonization of infrared radiation, which dominates in the X-ray band.

KEYWORDS: quasars, jets, nonthermal radiation

1. ASSUMPTIONS

• Nonthermal radiation in blazars is produced by thin shells, propagating at a constant relativistic ($\Gamma \gg 1$) speed along the conical jet;

• Relativistic electrons are injected in the shells within a distance range $\Delta r = r_0$, starting from r_0. They are injected at a constant rate and with the two power-law energy distribution, $Q = K\gamma^{-p}$ for $\gamma > \gamma_b$ and $Q \propto \gamma^{-1}$ for $\gamma \leq \gamma_b$;

• Radiative energy losses of electrons are dominated by Comptonization of the quasar broad emission lines. This process is responsible for production of γ-rays. The low energy break at few MeV results from inefficient radiation cooling of lower energy electrons;

• Intensity of the magnetic field is $B(r) = (r_0/r)B(r_0)$.

2. THE MODEL EQUATIONS

2.1. Electron Evolution

Evolution of the electron energy distribution is given by the continuity equation (Moderski, Sikora & Bulik 2000)

$$\frac{\partial N_\gamma}{\partial r} = -\frac{\partial}{\partial \gamma}\left(N_\gamma \frac{d\gamma}{dr}\right) + \frac{Q}{c\beta\Gamma}, \tag{1}$$

where

$$\frac{d\gamma}{dr} = \frac{1}{\beta c\Gamma}\left(\frac{d\gamma}{dt'}\right)_{rad} - \frac{2}{3}\frac{\gamma}{r}. \tag{2}$$

The second term on the rhs of Eq. (2) represents the adiabatic losses. The rate of the radiative energy losses is:

$$\left(\frac{d\gamma}{dt'}\right)_{rad} = -\frac{4\sigma_T}{3m_e c}(u'_B + u'_S + u'_{BEL} + u'_{IR})\gamma^2, \tag{3}$$

where $u'_B = B'^2/8\pi$ is the magnetic energy density, u'_S is the energy density of the synchrotron radiation field, $u'_{BEL} = (4/3)\Gamma^2 L_{BEL}/4\pi r^2 c$ is the energy density of the broad emission lines, $u'_{IR} \simeq (4/3)\Gamma^2 \xi_{IR} 4\sigma_{SB} T^4/c$ is the energy density of the near-IR radiation produced in molecular torus by hot dust, and ξ_{IR} is the fraction of the accretion disc radiation reprocessed by the dust into the near-IR band.

2.2. Radiation Spectra

The observed spectra as a function of time are computed using the formula

$$\nu L_\nu(t) \equiv 4\pi \frac{\partial(\nu L_\nu(t))}{\partial \Omega_{\vec{n}_{obs}}} = \iint_{\Omega_j} \frac{\nu' L'_{\nu'}[r(\theta,t),\theta]\mathcal{D}^4}{\Omega_j} \mathrm{d}\cos\theta \mathrm{d}\phi\,, \tag{4}$$

where $\mathcal{D} = [\Gamma(1-\beta\cos\theta)]^{-1}$ is the Doppler factor, $\nu = \mathcal{D}\nu'$, and $r = c\beta(t-t_0)/(1-\beta\cos\theta) + r_0$. The luminosity $\nu' L'_{\nu'}$ is contributed by: synchrotron radiation

$$\nu' L'_{S,\nu'} \simeq \frac{1}{2}(\gamma N_\gamma) m_e c^2 \left|\frac{\mathrm{d}\gamma}{\mathrm{d}t'}\right|_S. \tag{5}$$

the synchrotron-self-Compton (SSC) process

$$\nu' L'_{SSC,\nu'} = \frac{\sqrt{3}\sigma_T}{8\Omega_j r^2} \nu'^{3/2} \int N_\gamma \left[\gamma = \sqrt{\frac{3\nu'}{4\nu'_S}}\right] L'_{S,\nu'} \nu'^{-3/2}_S \,\mathrm{d}\nu'_S\,, \tag{6}$$

and the external-radiation-Compton (ERC) process

$$\nu' L'_{ERC,\nu'}[\theta'] \equiv 4\pi \frac{\partial(\nu' L'_{ERC,\nu'})}{\partial \Omega'_{\vec{n}'_{obs}}} \simeq \frac{1}{2}\gamma N_\gamma m_e c^2 \left|\frac{\mathrm{d}\gamma}{\mathrm{d}t'}\right|_{ERC}[\theta']\,, \tag{7}$$

where

$$\left|\frac{\mathrm{d}\gamma}{\mathrm{d}t'}\right|_{ERC}[\theta'] \simeq \frac{4\sigma_T}{3m_e c^2}\gamma^2 \mathcal{D}^2 (u_{BEL} + u_{IR})\,. \tag{8}$$

and

$$\nu' \simeq \mathcal{D}\gamma^2 \nu_{BEL/IR}\,, \tag{9}$$

where ν_{BEL} and ν_{IR} are average frequencies of broad emission lines and of infrared radiation of hot dust, respectively. Note that in the comoving frame the ERC radiation field is anisotropic, while the synchrotron and SSC radiation fields are isotropic (Dermer 1995).

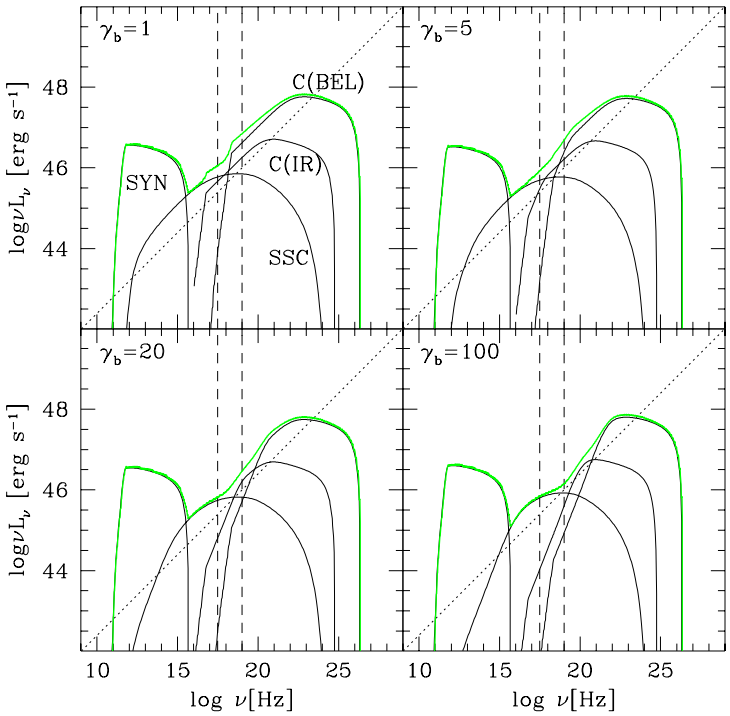

FIGURE 1. The time averaged blazar spectra for four values of γ_b. The dotted line marks the typical slope of the X-ray spectra in blazars ($\alpha = 0.6$); the dashed lines enclose the 1-30 keV X-ray band. In each panel we show four spectral components: synchrotron (SYN), synchrotron-self-compton (SSC), comptonization of broad emission lines [C(BEL)], and comptonization of near-IR dust radiation [C(IR)].

3. RESULTS

In Figure 1 we present the time averaged blazar spectra for four different values of the energy break γ_b. All models are computed for the following set of parameters: $r_0 = 6 \times 10^{17}$ cm; $\Gamma = 15$; $L_{BEL} = 1.4 \times 10^{44}$ ergs/s; $B' = 1.4$ Gauss; $\gamma_{max} = 10^4$; $p = 2.2$; $K = 0.7 \times 10^{50}$ s^{-1}; $\theta_{obs} = \theta_j = 1/15$ rad, $T = 1000$ K, and $\xi_{IR} = 0.08$. For the justification of this choice see Błażejowski et al (in preparation).

4. DISCUSSION

4.1. Low Energy Break in Electron Distribution

We can see from Fig. 1, that for $\gamma_b = 1$ the low energy tail of the C(BEL) component extends down to ~ 2 keV. Thus, any presence of thermal nonrelativistic electrons should be imprinted as a bump, peaking around 2 keV. Since blazar spectra extend

down to much lower values without any bump (Comastri et al. 1997; Sambruna 1997; Lawson & McHardy 1998), we exclude the domination of C(BEL) in the soft X-ray band.

In order to get soft X-ray spectra which smoothly join the middle X-ray band, one needs to assume that $\gamma_b > 3$. Then the low energy break of C(BEL) moves above > 20 keV and X-ray radiation below this value is dominated by either by SSC or C(IR). Noting that the SSC X-ray spectra are much softer than the observed ones ($\alpha_{X,SSC} \sim 1$ vs. $\alpha_{X,obs} \sim 0.6 - 0.7$; Kubo et al. 1998), C(IR) is a better candidate for X-ray production. This, however, can be the case if $\gamma_b \leq 10$. For larger values of γ_b the low energy break of the C(IR) component moves to energies > 20 keV, and, then, at lower energies the C(IR) spectrum becomes too hard in comparison with observations. We conclude that interpreting the blazar X-ray observations within the framework of our model implies that γ_b is enclosed in the range $(3 - 10)$.

4.2. Pair Content

For a jet dynamically dominated by the energy flux of protons, L_p, and for radiative energy losses of electrons dominated by Comptonization of broad emission lines, the pair content of the jet can be calculated from the formula (Sikora et al., in preparation)

$$\frac{n'_{pairs}}{n'_p} \sim \frac{K}{2(p-1)\gamma_b^{p-1}} \frac{m_p c^2}{L_p} \Gamma^2 \,, \tag{10}$$

This, for our model parameters and $3 < \gamma_b < 10$ gives

$$6/L_{p,47} < n'_{pairs}/n'_p < 26/L_{p,47} \,. \tag{11}$$

Thus, our results suggest that particle number in quasar jets is dominated by pairs, while the jet inertia is still dominated by protons.

ACKNOWLEDGEMENTS

This project was supported by ITP/NSF grant PHY94-07194, the Polish KBN grant 2P03D00415, and NASA grant NAG-5-6337.

REFERENCES

??omastri, A., Fossati, G., Ghisellini, G., & Molendi, S. 1997, ApJ, 480, 534

??ermer, C.D. 1995, ApJ, 446, L63

??awson, A.J., & M^{c}Hardy, I.M. 1998, MNRAS, 300, 1023

??ubo, H., et al. 1998, ApJ, 504, 693

??oderski, R., Sikora, M., Bulik, T., 2000, ApJ, in press

??ambruna, R.M. 1997, ApJ, 487, 536